Eur. Phys. J. E **14**, 169–175 (2004)
DOI 10.1140/epje/i2003-10147-x

THE EUROPEAN PHYSICAL JOURNAL E

Dynamic domain formation in membranes: Thickness-modulation–induced phase separation

E. Schäffer[1,a] and U. Thiele[2]

[1] Max Planck Institute of Molecular Cell Biology and Genetics, Pfotenhauerstraße 108, D-01307 Dresden, Germany
[2] Max-Planck-Institut für Physik komplexer Systeme, Nöthnitzer Straße 38, D-01187 Dresden, Germany

Received 22 December 2003 and Received in final form 26 March 2004 /
Published online: 15 July 2004 –

Abstract. A simple model investigates the amplification of fluctuations on membranes constituted of two lipids having different lengths. Van der Waals and electrostatic interactions across the lipid bilayer result in a destabilization favoring thickness variations of the membrane. Close to spontaneous demixing of the two components, the additional gain in free energy due to thickness undulations shifts the stability boundary which promotes phase separation into domains. Interestingly, this effect can be induced by an applied electric field or membrane potential. In biological systems, the dynamic model presented here indicates that electric fields might be important for controlling phase separation and the formation of domains called "rafts".

PACS. 87.16.Dg Membranes, bilayers, and vesicles – 68.35.Rh Phase transitions and critical phenomena – 82.70.Uv Surfactants, micellar solutions, vesicles, lamellae, amphiphilic systems, (hydrophilic and hydrophobic interactions)

1 Introduction

Biological membranes consist of many different lipids and proteins. Inherently, the heterogeneous nature of the lipid bilayer results in a complicated structure and rich physics [1,2]. Recent focus has been on the role and function of small lateral domains termed "rafts" [3–5]. These domains are enriched in sphingolipids and cholesterol and are supposed to be in the liquid-ordered state. In this phase, the mobility of the lipids is almost as high as in the liquid-disordered (liquid) state, however, their chains are extended and tightly packed. Consequently, these regions are thicker compared to the remaining glycerophospholipid-rich membrane [5–7]. Due to the expected small size of rafts and ensuant experimental difficulties in detecting them, little knowledge has been obtained on their size, interspacing, dynamics, and lifetime [5,8].

Interactions of membranes with external electric fields and inherent forces, for instance, van der Waals (vdW) forces, are important for membrane behavior and function (*e.g.*, bilayer repulsion) and their manipulation (*e.g.*, electroporation)[9,10]. Thermally excited undulations result in bending modes (analogous to the "buckling" instability) and peristaltic modes (thickness variations or "squeezing" modes) which couple to the above interactions. To describe such effects, idealized lipid bilayer systems are used as simple models.

[a] e-mail: Erik.Schaeffer@mpi-cbg.de

The theory applied to membranes was originally developed for viscous thin liquid films [11]. Hydrodynamic models have been fruitful in stability analyses of free-standing [11] or supported films [12]. Under certain conditions, a thickness modulation lowers the free energy of the system resulting in the break-up of the film. The competition between the stabilizing surface tension and destabilizing forces that act across the film normally selects a prominent initial mode with a characteristic wavelength. Experiments found great sensitivity of the interfaces and quantitative agreement with the models (regarding, *e.g.*, vdW forces, electric fields, temperature gradients, or acoustic fluctuations [13–18]). The effect of these interactions on heterogeneous films has received much less attention, due to the complexity of the systems.

Pertaining to membranes and their phases, bending undulations have been coupled to internal degrees of freedom resulting, for instance, in a curvature instability [2]. Spontaneous curvatures of membranes and liquid-crystal analogies have been used to explain the "ripple" phase occurring between the solid and liquid phases [19,20]. Charge-induced phase separation due to a variation of the ionic strength or the adsorption of ions has been studied for a long time [21,22]. Electric-field gradients in the plane of the membrane have been shown to cause local phase separation [23,24].

From a physical point of view, the notion of a raft could be explained in several ways. Regarding a binary mixture

of lipids, the membrane could either be in the one-phase or two-phase region. In the former, thermal fluctuations in composition could account for domain formation. Corresponding correlation lengths and times depend on how far the system is away from its critical point. Only very close to the critical point would correlation times and lengths be sufficient to account for biological measures of rafts (on the order of several tens of nanometers) [5,8,20]. If the system is in a two-phase region, macroscopic phase separation is expected in thermodynamic equilibrium. This is often observed in model membranes [5]. Alternatively, in a ternary mixture, the minority component could act as a surfactant and reduce the interfacial energies between domains resulting in a stable micro-emulsion because of entropic reasons (*e.g.*,[25]). Finally, in the absence of thermodynamic equilibrium, the dynamics of phase separation after a quench from a one-phase to a multi-phase region results in domain formation. After an initial (fast) period of spinodal decomposition, the (slow) growth (Ostwald ripening) and coalescence of domains determines the size distribution and lifetime of domains [26]. In this case, the presence of a surfactant reduces the domain size [27] and stabilizes the system inhibiting domain growth and coalescence [26, 28]. Biological membranes are composed of many (> 200) different lipids and are thought to be near phase separation boundaries [23]. Cholesterol plays a key role in determining function and physical properties of membranes [1, 29]. In order to get a grip on the complexity of membranes, one step is to map multi-component mixtures containing cholesterol onto a binary system [30].

In analogy to the thin-film experiments, changes in membrane thickness can lower the free-energy contributions of electrostatic and long-range forces across the membrane. This gain in energy can in turn induce a phase separation in the membrane resulting in the formation of domains. The conditions under which such a phase separation can occur and the relevance to biological systems are discussed in this paper. In Section 2, we present a two-component model which focusses on dynamic domain formation after a quench from the one-phase to the two-phase region. In a system that shows phase separation and which is already close to spontaneous demixing, varying an additional degree of freedom —the membrane thickness— can lower the overall free energy and demix the lipids. While van der Waals forces inherently change with the membrane thickness, changing an external electric field applied across the membrane leads to the novel aspect that this coupling can actively support and regulate phase separation. Section 3 illustrates the model predictions regarding initial domain size, characteristic spacing and temporal characteristics. The concluding Section 4 interprets the implications of our model for multi-component biological systems.

2 Model

The simplest possible membrane model assumes a two-component mixture (Fig. 1). Each component i ($i = 1, 2$) has a concentration (area fraction) c_i in the membrane

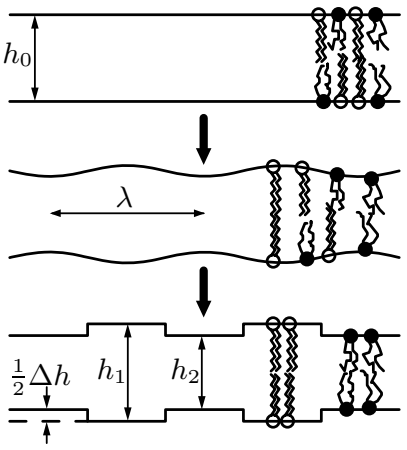

Fig. 1. Schematic drawing of a membrane composed of two components. In the one-phase region, the membrane has a thickness h_0 (top). If the system is quenched into the two-phase region, the membrane phase separates via a spinodal decomposition with characteristic wavelength $\lambda = 2\pi q^{-1}$ (q: wave number, middle) into two phases with thicknesses h_1 and h_2 (bottom).

with $c_1 + c_2 = 1$. For simplicity, we assume that the area per molecule of the two components is equal, that the spontaneous curvature of the mixture and its phases is negligible [31,32], and that the components are in a liquid state. The latter two assumptions are motivated by experimental systems mimicking biological membranes that show a liquid-order–to–disorder transition. The system is described by a phenomenological Ginzburg-Landau functional $\mathcal{F}$ corresponding to an energy per unit area. We choose the order parameter to be $c \equiv c_1$. The expansion of this functional with respect to the concentration is given by [2]

$$\mathcal{F}_c = \frac{1}{2} B_e \left(\nabla c\right)^2 + f_c(c). \tag{1}$$

The first term describes the increase in energy due to concentration gradients with the effective interaction parameter $B_e > 0$ between domains. The local term $f_c(c)$ can be interpreted as the free energy per unit area of a membrane with a homogeneous thickness. The dependence of the free energy on the concentration for the binary mixture of the two different lipids is approximated by [33]

$$f_c(c) = \frac{w}{a} c(1-c) + \frac{kT}{a} \left[c \ln c + (1-c) \ln(1-c)\right]. \tag{2}$$

k is Boltzmann's constant, T the temperature, a is the area per molecule, and w is an interaction parameter. This is a mean-field theory with a critical mixing point at $c_c^0 = 0.5$ and $w = 2kT_c^0$. The condition $\partial_{cc} f_c = 0$ (where ∂_c denotes the partial derivative with respect to c) determines the spinodal to be at $T_s^0 = 4T_c^0\, c(1-c)$. It corresponds to the boundary between the one-phase and the two-phase region.

If the two lipids making up the membrane have different lengths, the membrane has another degree of freedom:

the membrane thickness. Therefore, the total free energy is given by

$$\mathcal{F} = \mathcal{F}_c + \mathcal{F}_h \tag{3}$$

where $\mathcal{F}_h$ is the free energy related to thickness variations. Instead of introducing additional coupling terms, which only lead to higher-order corrections, and solving a set of coupled equations, the inherent nature of the system simplifies matters. The order parameters c and h are not independent. The fluid-like packing of lipid tails implies volume conservation which imposes a direct coupling of c and h. In pure form each component has a height h_i. The area per head group is assumed to remain constant while the lipid tails are allowed to be flexible. In the one-phase region, the membrane thickness h, in a first-order approximation, is then given by

$$h = c_1 h_1 + c_2 h_2. \tag{4}$$

All variables are mean-field quantities meaning that they are averages over distances large compared with the lateral dimensions of the lipids. This assumes that the conformation of the tails plays no role as long as the mean density remains constant. Equation (4) can be rewritten in a form that shows that a change in local lipid concentration invokes a change in the membrane thickness

$$h = h_0 + \Delta h(c - c_0), \tag{5}$$

where $\Delta h = h_1 - h_2$ is the difference in membrane thickness (see Fig. 1), c_0 is the initial concentration of component 1, and $h_0 = c_0 h_1 + (1 - c_0)h_2$ is the equilibrium membrane thickness in the one-phase region. The contribution of the thickness variations to the free energy is

$$\mathcal{F}_h = \frac{1}{4}\gamma \left(\nabla h\right)^2 + f_h(h) \tag{6}$$

with the surface energy γ. The first term accounts for an increase in surface area. The second term, $f_h(h) = f_{\mathrm{vdW}} + f_{\mathrm{el}} + \ldots$, contains all membrane spanning interactions that depend on the membrane thickness. Most prominent are the changes in the vdW interactions of the aqueous half-spaces across the hydrocarbon membrane. The nonretarded vdW potential is given by [9]

$$f_{\mathrm{vdW}} = -\frac{A}{12\pi h^2}, \tag{7}$$

with the Hamaker constant A that depends on the dielectric properties of the two half-spaces above and below and on the membrane itself. Compared to free membranes, the Hamaker constant can change drastically for supported bilayers [9,34].

Additionally, we take into account the contribution of an externally applied electric field across the membrane which could mimic a biologically relevant potential. To our knowledge, this term has been considered in the context of electroporation but not with respect to phase separation. The electrostatic interactions are in a long-wavelength limit (membrane thickness small compared to lateral length scales) approximated by

$$f_{\mathrm{el}} = -\frac{\varepsilon_0 \varepsilon \Delta V^2}{2h}, \tag{8}$$

where ε_0 is the vacuum permittivity, ε the dielectric constant of the hydrocarbon bilayer, and ΔV the absolute value of the membrane potential. A high ionic strength (physiological conditions) is assumed such that the membrane potential acts essentially across the membrane thickness, *i.e.* all screening lengths are much smaller than the membrane thickness [15]. The effect of surface charges (charged lipids) has been studied extensively (*e.g.*, [21]). A recent study has shown, however, that the Coulomb repulsion of the excess charges leading to a long-wavelength instability is compensated by a correlated charge fluctuation and furthermore is screened by free ions in solution [35]. Therefore, we only take into account the effect of an external membrane potential with uncharged lipids. To exclude effects of demixing due to lateral field gradients, we assume that there is no difference in the dipole moment density of the lipids [24]. Because we are interested in a redistribution of molecules in the membrane we do not consider any elastic (bending (see note [32]) or compressional energies) and steric effects.

Generally, the dielectric properties of two lipids are different causing membrane properties to depend on the concentration, $\varepsilon(c)$ and $A(c)$. In addition, the interaction parameter in equation (2) may depend on the thickness, $w(h)$. These dependencies result in coupling terms in equation (3). However, with the above assumptions the dielectric properties differ mainly in the lipid head group. Therefore, we assume that differences are small and use constant parameters ε, A and w.

The time evolution of the membrane composition $c = c(x,t)$ is given by the continuity equation

$$\partial_t c = -\partial_x j, \tag{9}$$

where j is the flow of lipids through the cross-section of the membrane, t is the time, and ∂_t (∂_x) denotes the partial derivative with respect to t (x). We simplified the problem to one lateral coordinate x. In a non-equilibrium situation, gradients of the generalized chemical potential ($\mu = \frac{\delta \mathcal{F}}{\delta c}$ given by the variational derivative of the total free energy with respect to the concentration) provide the driving force for the lipids' movement. The current density (flux of component 1) is given by

$$j = -M\partial_x \frac{\delta \mathcal{F}}{\delta c}, \tag{10}$$

where M is a mobility which could be concentration dependent. The equation of motion relevant for the system results from combining equation (9) and equation (10):

$$\partial_t c = \partial_x \left[M \partial_x \left(\frac{\delta \mathcal{F}}{\delta c} \right) \right]. \tag{11}$$

Note that due to equations (3) and (5), $\mathcal{F} = \mathcal{F}[c, h(c)]$. The form of equation (11) is common and well studied for conserved systems [36].

A linear stability analysis determines whether small composition fluctuations present due to thermal fluctuations $c\,(x,t) = c_0 + \varsigma \exp\left(iqx + t/\tau\right)$ with wave number q (see Fig. 1) and amplitude ς will be exponentially

amplified (growth rate $\tau^{-1} > 0$) or damped ($\tau < 0$). Here, we concentrate on peristaltic modes since bending modes in this approximation do not lower the free energy with regard to vdW and electrostatic interactions (bending modes would correspond to a ripple phase [19]). This is already implied by equation (5), tacitly assuming that the two leaflets of the membrane are coupled. The dispersion relation is

$$\frac{1}{\tau} = -M_0 \left(Bq^4 + Cq^2 \right). \tag{12}$$

The mobility parameter M_0 is constant during the linear stage. For an estimation of M_0 see the appendix. $B = B_e + \Delta h^2 \gamma/2$ and composed of the edge energy B_e plus a surface energy term due to an increase in surface area for an undulated interface. The coefficient C determines the stability of the membrane

$$\begin{aligned} C &= \partial_{cc} f_c\big|_{c=c_0} + \Delta h^2 \partial_{hh} f_h\big|_{h=h_0} \\ &= \alpha - \left[\frac{A}{2\pi h_0^4} + \frac{\varepsilon_0 \varepsilon \Delta V^2}{h_0^3} \right] \Delta h^2, \end{aligned} \tag{13}$$

where we have introduced the parameter $\alpha = \frac{2w}{a}\Theta$ with the reduced temperature $\Theta = (T - T^\star)/T^\star$ and $T^\star = 4c_0(1-c_0)T_c^0$. $C = 0$ gives the new spinodal with the associated temperature

$$T_s(c) = T_s^0 \left(1 - \frac{\Delta h^2 a}{4kT_c^0} \partial_{hh} f_h \right). \tag{14}$$

Since $\partial_{hh} f_h[h(c)] < 0$ the spinodal is shifted asymmetrically to higher temperatures with the maximum (critical point) shifted to $c < 0.5$. The shift of the spinodal depends quadratically on the thickness difference between the components. In the case that C is negative, all modes with $q < q_c$ are amplified. The fastest growing mode q_m is then given by

$$q_m^2 = \frac{1}{2} q_c^2 = -\frac{C}{2B} \tag{15}$$

with the associated growth rate

$$\frac{1}{\tau_m} = M_0 B q_m^4. \tag{16}$$

The free-energy gain per unit area for an unstable membrane is calculated by

$$\Delta \mathcal{F}_u = \frac{1}{\lambda} \int_0^\lambda (\mathcal{F}_u - \mathcal{F}_i)\, \mathrm{d}x \tag{17}$$

where the subscripts correspond to the undulatory state (u) sketched in the middle of Figure 1 and the initial planar membrane (i, Fig. 1 top). Up to second order in the fluctuation amplitude ς the calculation yields for the fastest growing mode

$$\Delta \mathcal{F}_u = -\frac{1}{4} \varsigma^2 B q_m^2. \tag{18}$$

Depending on the relative strength of the terms in equation (13) one can distinguish four cases. For $C > 0$ all time constants are negative; fluctuations are damped. If $C = 0$, the coefficient α has to be positive and compensate the vdW and electrostatic pressure gradients. For negative values of C, the membrane becomes unstable and fluctuations are exponentially amplified. One can distinguish between $\alpha < 0$ and $\alpha \geq 0$. The latter case is the most interesting: For a small $\alpha > 0$, which corresponds to the one-phase region of a system with $\Delta h = 0$, when $\Delta h \neq 0$, the system can be shifted to the two-phase region ($C < 0$). Close to the spinodal, an otherwise homogeneous membrane can phase separate due to the inter-membrane potentials. vdW interactions are usually constant, however, a small change in the membrane potential could induce the effect. A sufficient change in ΔV can invert the sign of C corresponding to a quench from the one-phase to the two-phase region. The change in ΔV is analogous to typical phase separation experiments where T is varied.

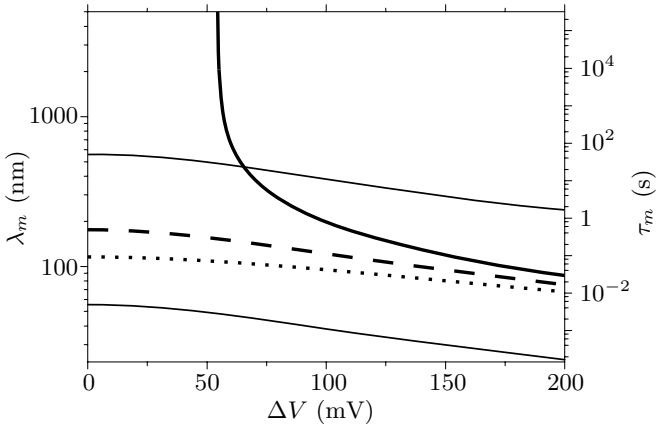

Fig. 2. Characteristic wavelength $\lambda_m = 2\pi q_m^{-1}$ (Eq. (15)) as a function of the (absolute) membrane potential ΔV. The thick lines use $\gamma_{\text{eff}} = 1\,\text{mNm}^{-1}$ and the reduced temperature $\Theta = 0$ ($\alpha = 0$, dashed), $\Theta = +5 \cdot 10^{-5}$ (solid), and $\Theta = -5 \cdot 10^{-5}$ (dotted). The characteristic time scale τ_m for the same curves (thick lines) plotted on the right-hand side is related to λ_m by equation (16). The thick solid line diverges for a certain critical voltage $\Delta V_c \approx 55\,\text{mV}$ indicating stability of the system for $\Delta V < \Delta V_c$. The thin lines are characterized by $\alpha = 0$ and $\gamma_{\text{eff}} = 0.1\,\text{mNm}^{-1}$ (lower thin line) and $10\,\text{mNm}^{-1}$ (upper thin line) showing the effect of changing the interfacial energies. The time scale does not apply to the thin curves. For remaining parameters see the main text.

3 Results

The results and conditions of the dynamic instability after a quench are illustrated in Figure 2 (explained in detail below). To estimate the order of magnitude of the effect, parameters corresponding to physiological conditions are chosen. A rough estimate for B can be obtained from the typical interfacial energy γ between different hydrocarbons (polymers) which is about $1\,\text{mNm}^{-1}$ [37]. The edge energy between two different lipids in direct contact can be approximated by their surface free energy

times the contact area (height of the membrane times the lipid diameter) $B_e \approx 2hr\gamma$. As a typical membrane thickness we use $h_0 = 5\,\mathrm{nm}$ with a radius for a single lipid of $r \approx 0.5\,\mathrm{nm}$ [6,9]. The difference in height of domains formed in a ternary mixture of glycerophospholipids, sphingolipids, and cholesterol has been measured by atomic force microscopy (AFM) to be $\Delta h \approx 0.8\,\mathrm{nm}$ [6,7]. Studies on ternary polymer films [28,26,27] and computer simulations on ternary lipid systems [38] and binary lipid systems with added cholesterol [1], indicate that cholesterol acts as a surfactant. Since a surfactant can lower the interfacial energies by orders of magnitude, our estimate for B_e is an upper bound (see also note [39]). It is useful to introduce an effective surface energy $\gamma_{\mathrm{eff}} = (4hr/\Delta h^2 + 1)\gamma = 2B/\Delta h^2$.

As the Hamaker constant for a water-hydrocarbon-water system is in the range of $4\text{–}7{\cdot}10^{-21}\,\mathrm{J}$ we chose an intermediate value of $A = 5 \cdot 10^{-21}\,\mathrm{J}$ [9]. Common membrane potentials (absolute values) are on the order of several tens of millivolts. Macroscopically, this may appear insignificant, however, across the thin membrane acting as an insulator with a dielectric constant of $\varepsilon \approx 2$, the potential drop results in an electric field on the order of $10^7\,\mathrm{V\,m^{-1}}$.

In Figure 2 the characteristic wavelength $\lambda_m = 2\pi q_m^{-1}$ (left-hand axis, Eq. (15)) and the time τ_m (right-hand axis, Eq. (16), see appendix) is plotted as a function of the (absolute) membrane potential for a representative value of $\gamma_{\mathrm{eff}} = 1\,\mathrm{mNm^{-1}}$. λ_m corresponds to the typical spacing between domains and τ_m gives an estimate for the time it takes to form a domain. At the "old" spinodal in the absence of thickness undulations ($\alpha = \Theta = 0$, dashed line), the membrane is now unstable due to the inter-membrane potentials. λ_m is on the order of 100 nm with a time constant of around 100 ms. Moving away from this point to the most interesting situation mentioned at the end of Section 2 (thick solid line: $\Theta = 5 \cdot 10^{-5}$ corresponding to $T - T^\star = 1.55 \cdot 10^{-2}\,\mathrm{K}$ with $T^\star = 310\,\mathrm{K}$), the membrane becomes stable below a critical voltage $\Delta V_c \approx 55\,\mathrm{mV}$, where the parameter C is positive (see Eq. (13)). For comparison λ_m is plotted for $\Theta = -5 \cdot 10^{-5}$ (dotted line). The curves for $\gamma_{\mathrm{eff}} = 0.1$ and $10\,\mathrm{mNm^{-1}}$ (thin solid lines using $\Theta = 0$, the time scale does not apply here) show the effect of varying the interfacial energies. Thus in a biological system close to spontaneous demixing, the cell membrane could be switched from a one-phase state (no "rafts") to a two-phase ("raft") state by increasing the membrane potential above ΔV_c and vice versa. ΔV is the control parameter of the system by which a quench into the two-phase region can be realized. Alternative control parameters are discussed below. An initial concentration of $c_0 \approx 0.5$ results in a domain size ($c_0\lambda_m$) on the order of 50 nm which compares well with experimental results [8,5].

A temperature difference of 16 mK away from the spinodal might seem small. However, due to the simplifications in the model the equations can at best give the correct order of magnitude for the results. The range of chosen parameters also has an influence. For instance, changing the parameters to a different set of still reasonable values ($A \approx 1 \cdot 10^{-20}\,\mathrm{J}$, $\varepsilon = 2.5$, $h_0 = 4\,\mathrm{nm}$, $\Delta h \approx 1\,\mathrm{nm}$, $r \approx 0.55\,\mathrm{nm}$) while keeping the above ΔV_c yields a temperature difference of $\approx 0.12\,\mathrm{K}$.

The functional relationship of equation (15) is qualitatively seen in experiments of supported mono- and bilayers [7]. For monolayers h_0 and Δh are only half of the bilayer values. This should decrease λ_m which is borne out by the experiments. Furthermore, upon addition of cholesterol to a two component lipid mixture the characteristic spacing between domains is reduced indicating the surfactant character of cholesterol.

Equation (18) can be used for a rough estimate of the free-energy gain $\Delta E = \Delta\mathcal{F}_u\lambda_m^2$ for the characteristic mode. Using $\gamma_{\mathrm{eff}} \approx 1\,\mathrm{mNm^{-1}}$, $\varsigma = 0.5$ (corresponding to a height difference Δh between domains), and $\lambda_m \approx 100\,\mathrm{nm}$, the free-energy gain for the fastest growing mode is on the order of kT. This means that even for $\Theta \geq 0$ and $C < 0$, the system does not show a macroscopic phase separation since thermal fluctuations compete with coarsening by mixing the system again. Since the gain in free energy is about kT, driving forces are comparable to Langevin forces which cause the Brownian motion of lipids. Thus, equation (11) has to be modified to include a term accounting for random fluctuations [40]. The critical wave number is then determined by the balance between thermal and thermodynamic driving forces. Assuming that the system has only two states, the initial flat and an undulated one (with a typical wavelength λ_m), we can use Boltzmann's law to calculate the ratio of probabilities of being in either state. Using the above values, $\Delta E \approx -0.2\,\mathrm{kT}$ and $p_u/p_i = \exp(-\Delta E/kT) \approx 1.22$ where the probabilities for the undulated and the initial flat state, respectively, fulfil $p_u + p_i = 1$. Therefore, the probability of being in the phase-separated state for the chosen parameters is $\approx 55\%$. Since the gain in free energy of a coarsening process is much smaller than that of the initial formation of the unstable mode, the probability of a coarsened mode is rather small, even for the first coarsening step from a typical length λ_m to $2\lambda_m$. In other words, the system does not show a macroscopic phase separation because thermal fluctuations remix the system.

4 Final remarks

The schematic ternary-phase diagram in Figure 3 (adapted from Silvius *et al.* [41]) shows the range of typical biological membrane mimicking compositions [4]. Such mixtures have recently been shown to exhibit "raft"-like domains under physiological conditions [42]. Relative concentrations of glycerophospholipid (GPL), cholesterol (Chol), and sphingolipid (SL) marking the boundary (solid line) between liquid-ordered (l_o) and -disordered (l_d) phases are illustrated. If for example a membrane has a composition as marked by the circle which is in the l_d phase, a change in the membrane potential could render the point in the two-phase region as indicated by the dashed line (the spinodal is shifted, exaggerated in the schematic). Subsequently, the above described dynamic instability would set in. Alternatively, an increase in the

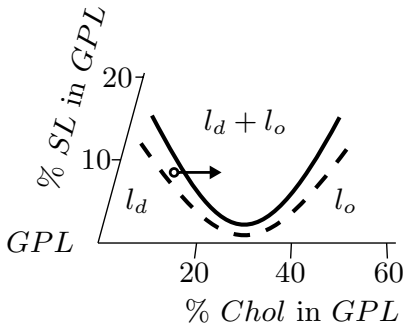

Fig. 3. Schematic ternary-phase diagram adapted from Silvius *et al.* [41] showing the concentration ranges and phases of physiological membranes. Relative concentrations of a sterol (cholesterol, Chol) and a sphingolipid (SL) in a glycerophospholipid (GPL) are indicated on the axes. The spinodal (solid line) between liquid-disordered (l_d) and liquid-ordered (l_o) phases is lowered by the inter-membrane potentials (dashed line, shift exaggerated).

cholesterol concentration (arrow in Fig. 3) would also position the membrane in the unstable region. Instead of varying the temperature, a change in the surface pressure can place the membrane close to the spinodal (*e.g.*, [30]). Within a cell, membrane tension can for example be regulated by the ion concentrations resulting in changes of the osmotic pressure. In case of large temperature changes, the cell can therefore adapt the membrane tension to ensure proximity to the phase transition. Once the system is close to the transition, a cell possesses fast means using ion channels to switch between stable and unstable states by changing the membrane potential. The vdW and electrostatic interactions therefore have a special role because they interact with the membrane via an independent degree of freedom —the membrane thickness. Especially, the electrostatic interactions enable the cell to rapidly control its membrane state by other means than changing the temperature or pressure which usually takes place on a long time scale.

The vdW and electrostatic interactions have further consequences. The thickness modulation also means that the bilayer is coupled. This effect has also been attributed to the presence of cholesterol [6] and is controversial [43]. The electric field polarizes the membrane. Thickness variations result in lateral electric-field gradients. If the two components have different dipole moment densities, the phase separation is enhanced [23]. Since our system is vastly simplified, other effects not included could play an important role in biological membranes. For example, the presence of proteins could act as nucleation sites [5, 44]. Such heterogeneous nucleation could dominate over the homogeneous spinodal decomposition mechanism discussed here [45,46].

In conclusion, we have shown that forces in membranes stemming from van der Waals and electrostatic interactions across the membrane may, under certain conditions, lead to a phase separation resulting in domains. Especially, the coupling of thickness undulations to electric fields has thus far been neglected and could be relevant in biological systems. The energy gain due to a thickness modulation is comparable to the energy associated with thermal fluctuations. A macroscopic phase separation is therefore not expected. The dynamic model predicts a characteristic spacing between domains on the order of 100 nm. This parameter and its scaling behavior with respect to, *e.g.*, the membrane potential has not been measured experimentally, yet. An AFM study of supported bilayers, mimicking biological membranes, with the substrate, composition, and temperature adjusted to poise the membrane close to the spinodal should show the transition from a homogeneous to a phase-separated state upon applying an electric field across the membrane. Such an experiment could clarify whether "rafts" are a manifestation of a phase separation process.

We would like to thank M. Bär, J. Helenius, J. Howard, K. John, F. Jülicher, K. Simons, and U. Steiner for discussions and help with the manuscript. This work was funded by the Max Planck Institute of Molecular Cell Biology and Genetics, Dresden, Germany.

Appendix A. Mobility approximation

One can get a crude approximation of the mobility parameter and derive how the current j is related to the chemical potential pressure gradient in the following manner. We model two opposing lipid molecules in the bilayer as a cylinder with radius r and height h_0 spanning the membrane [47]. The viscosity of the membrane is assumed to be much larger than that of the surrounding fluids. The force acting on the cylinder due to the linear lateral hydrostatic-pressure gradient is obtained by integrating the local pressure contributions over the mantel of the cylinder a exposed to the pressure $p(x)$ in the membrane

$$F_p = \oint p(x)\mathrm{d}a = \pi h r^2 \partial_x p. \tag{A.1}$$

F_p is opposed by the viscous drag force on the cylinder $F_{\mathrm{vis}} = \Gamma v$, where Γ is the drag coefficient and v the velocity of the cylinder. The drag coefficient is related to the diffusion constant D by Einstein's relation $D = kT/\Gamma$ (k Boltzmann constant). The (volume) flow in the membrane is $j_h = hv$. Putting everything together yields

$$j_h = -\frac{Dh^2}{\tilde{\alpha}}\partial_x p, \tag{A.2}$$

where we have introduced the parameter $\tilde{\alpha} = \frac{kT}{\pi r^2}$. The diffusion coefficient is assumed to be similar for all involved components. The hydrostatic pressure in the film is given by the variational derivative of the total free energy with respect to the membrane thickness, $p = \frac{\delta \mathcal{F}}{\delta h}$ which, for $\Delta h \neq 0$, is $\frac{\delta \mathcal{F}}{\delta h} = \frac{1}{\Delta h}\frac{\delta \mathcal{F}}{\delta c}$. The flow of lipids is related to the volumetric flow by $j = j_h/h$. Equation (A.2) becomes

$$j = -\frac{Dh}{\tilde{\alpha}\Delta h}\partial_x \frac{\delta \mathcal{F}}{\delta c}. \tag{A.3}$$

Comparing equation (10) with equation (A.3) and setting $h = h_0$ for the linear stage, the mobility parameter is identified by

$$M_0 = \frac{Dh_0}{\tilde{\alpha}\Delta h}. \tag{A.4}$$

Since cholesterol is one of the key components in raft formation, we have chosen its diffusion constant at $T = 310\,\mathrm{K}$, $D \approx 3.4 \cdot 10^{-12}\,\mathrm{m^2\,s^{-1}}$ [48]. This value (order of magnitude) is also typical for lipids [49]. The mobility parameter is then approximately $M_0 \approx 3.9 \cdot 10^{-9}\,\mathrm{m^4(J\,s)^{-1}}$.

References

1. M. Bloom, E. Evans, O.G. Mouritsen, Quart. Rev. Biophys. **24**, 293 (1991).
2. S. Leibler, in *Jerusalem Winter School for Theoretical Physics*, Vol. **5** - *Statistical Mechanics of Membranes and Surfaces*, edited by D. Nelson, T. Piran, S. Weinberg (World Scientific, Singapore, 1989) pp. 45-103.
3. K. Simons, E. Ikonen, Nature **387**, 569 (1997); K. Simons, W.L.C. Vaz, Annu. Rev. Biophys. Biomol. Struct. **33**, 269 (2004).
4. D.A. Brown, E. London, J. Membrane Biol. **164**, 103 (1998).
5. C. Yuan, J. Furlong, P. Burgos, L.J. Johnston, Biophys. J. **82**, 2526 (2002).
6. H.A. Rinia, M. Snel, J. van der Eerden, B. de Kruijff, FEBS Lett. **501**, 92 (2001).
7. J.C. Lawrence, D.E. Saslowsky, J.M. Edwardson, R.M. Henderson, Biophys. J. **84**, 1827 (2003).
8. A. Pralle, P. Keller, E.-L. Florin, K. Simons, J.K.H. Hörber, J. Cell Biol. **148**, 997 (2000).
9. J.N. Israelachvili, *Intermolecular and Surface Forces* (Academic Press, London, 1991).
10. M.B. Partenskii, V.L. Dorman, P.C. Jordan, J. Chem. Phys. **109**, 10361 (1998).
11. A. Vrij, Discuss. Faraday Soc. **42**, 23 (1966).
12. E. Ruckenstein, R.K. Jain, J. Chem. Soc. Faraday Trans. II **70**, 132 (1974).
13. R. Seemann, S. Herminghaus, K. Jacobs, Phys. Rev. Lett. **86**, 5534 (2001).
14. E. Schäffer, T. Thurn-Albrecht, T.P. Russell, U. Steiner, Europhys. Lett. **53**, 518 (2001).
15. S. Herminghaus, Phys. Rev. Lett. **83**, 2359 (1999).
16. E. Schäffer, S. Harkema, R. Blossey, U. Steiner, Europhys. Lett. **60**, 255 (2002).
17. E. Schäffer, U. Steiner, Europhys. J. E **8**, 347 (2002).
18. U. Thiele, M. Mertig, W. Pompe, Phys. Rev. Lett. **80**, 2869 (1998).
19. M. Marder, H.L. Frisch, J.S. Langer, H.M. McConnell, Proc. Natl. Acad. Sci. U.S.A. **81**, 6559 (1984).
20. T. Heimburg, Biophys. J. **78**, 1154 (2000).
21. E. Sackmann, in *Handbook of Biological Physics*, Vol. **1A** - *Structure and Dynamics of Membranes*, edited by R. Lipowsky, E. Sackmann (Elsevier, Amsterdam, 1995) pp. 213-304.
22. G.D. Guttman, D. Andelman, J. Phys. II **3**, 1411 (1993).
23. K.Y.C. Lee, H.M. McConnell, Biophys. J. **68**, 1740 (1995).
24. A. Radhakrishnan, H.M. McConnell, Proc. Natl. Acad. Sci. U.S.A. **97**, 1073 (2000).
25. G. Gompper, M. Schick, in *Phase Transitions and Critical Phenomena*, edited by C. Domb, J.L. Lebowitz, Vol. **16** (Academic Press, London, 1994).
26. A.P. Russo, E.B. Nauman, J. Polym. Sci. B **38**, 1301 (2000).
27. S. Walheim, M. Ramstein, U. Steiner, Langmuir **15**, 4828 (1999).
28. E. Nauman, D. He, Polymer **35**, 2243 (1994).
29. L. Miao, M. Nielsen, J. Thewalt, J.H. Ipsen, M. Bloom, M.J. Zuckermann, O.G. Mouritsen, Biophys. J. **82**, 1429 (2002).
30. T.G. Anderson, H.M. McConnell, J. Phys. Chem. B **104**, 9918 (2000).
31. T. Baumgart, S.T. Hess, W.W. Webb, Nature **425**, 821 (2003).
32. The spontaneous curvature is neglected in [31] because the equilibrated vesicles mimicking biological membranes show bilayer inversion symmetry. The bending energy per area is $\mathcal{F}_b = \frac{1}{2}\kappa(2R^{-1} - R_0^{-1})^2$ (κ: bending rigidity, R (R_0): principal (spontaneous) radius of curvature). Estimating the energy contribution by $\Delta E_b \approx \mathcal{F}_b\lambda_m^2$ with $\kappa = 10^{-19}\,\mathrm{J}$, $R = 10\,\mu\mathrm{m}$ (from [31]), and $\lambda_m = 100\,\mathrm{nm}$ $\Delta E_b \approx 5 \cdot 10^{-3}kT$. Since $R \ll R_0$ the spontaneous curvature should contribute even less to the overall energy in our case.
33. J.W. Cahn, J.E. Hilliard, J. Chem. Phys. **28**, 258 (1958).
34. P.S. Swain, D. Andelman, Phys. Rev. E **63**, 51911 (2001).
35. Y.W. Kim, W. Sung, Europhys. Lett. **58**, 147 (2002).
36. J.S. Langer, in *Solids far from Equilibrium*, edited by C. Godreche (Cambridge University Press, 1992) Chapt. 3, pp. 297-363.
37. Z. Lin, T. Kerle, T.P. Russell, E. Schäffer, U. Steiner, Macromolecules **35**, 3971 (2002).
38. L.K. Nielsen, A. Vishnyakov, K. Jørgensen, T. Bjørnholm, O.G. Mouritsen, J. Phys. Condens. Matter **12**, A309 (2000).
39. Close to demixing the line tension $B_e/(2r)$ is expected to decrease. Recent experimental values [31] indicate up to two-orders-of-magnitude lower values compared to our conservative estimate.
40. H.E. Cook, Acta Metall. **18**, 297 (1970).
41. J.R. Silvius, D. d. Giudice, M. Lafleur, Biochem. **35**, 15198 (1996). For more quantitative information see, R.F.M. de Almeida, A. Fedorov, M. Prieto, Biophys. J. **85**, 2406 (2003).
42. J.R. Silvius, Biophys. J. **85**, 1034 (2003).
43. T.-Y. Wang, J.R. Silvius, Biophys. J. **81**, 2762 (2001).
44. J.C. Owicki, H.M. McConnell, Proc. Natl. Acad. Sci. U.S.A. **76**, 47 (1979).
45. U. Thiele, M.G. Velarde, K. Neuffer, Phys. Rev. Lett. **87**, 16104 (2001).
46. U. Thiele, K. Neuffer, Y. Pomeau, M.G. Velarde, Colloid Surf. A **206**, 135 (2002).
47. P.G. Saffman, M. Delbrück, Proc. Natl. Acad. Sci. U.S.A. **72**, 3111 (1975).
48. G. Orädd, G. Lindblom, P.W. Westerman, Biophys. J. **83**, 2702 (2002).
49. J. Korlach, P. Schwille, W.W. Webb, G.W. Feigenson, Proc. Natl. Acad. Sci. U.S.A. **96**, 8461 (1999).